

Appendix J, Winter and Spring Pulses and Delta Outflow

Attachment J.1 Longfin Smelt Outflow

J.1.1 Model Overview

The potential effect of operations on Longfin Smelt abundance was investigated through development of a statistical modeling approach relating the Longfin Smelt Fall Midwater Trawl (FMWT) abundance index to: (1) Delta outflow¹; (2) the FMWT abundance index two years earlier (as a representation of parental stock size), and; (3) ecological regime (i.e., 1967–1987, pre-*Potamocorbula amurensis* invasion; 1988–2002, post-*P. amurensis* invasion; and 2003–2022, Pelagic Organism Decline [POD]). The inclusion of the regime factor represents major ecological change points in the Bay-Delta (e.g., Nobriga and Rosenfield 2016; Sommer et al. 2007). Total Delta outflow (thousand acre-feet) was summed and examined as an explanatory covariate for two overlapping time periods: December through May, and March through May. Similar time periods have also been investigated in previous studies by Mount et al. (2013:66–69) and Nobriga and Rosenfield (2016). Bayesian methods were used to account for model uncertainty (e.g., uncertainty in the time period over which Delta Outflow is considered to affect Longfin Smelt abundance), therefore integrating an important component of scientific uncertainty into the resulting model predictions for decision making.

J.1.2 Model Development

J.1.2.1 Methods

Twelve log-linear regression models were considered in the analysis. The models were fit to the FMWT index of Longfin Smelt abundance² (1967–2022) using a Bayesian approach implemented in the R statistical computing language (R Core Team 2023) via the *brms* package (Bürkner 2017). Three Markov Chain Monte Carlo chains were run for each model and flat priors were assumed for covariates. There was a 2,000-sample warm-up for each chain before 10,000 samples were retained as draws from the posterior (30,000 samples total drawn from the posterior). Bayesian values for the \hat{R} statistic were less than 1.01 across estimated parameters, which indicated sampling converged on the posterior probability distributions for all models considered.

¹ Downloaded from: <https://data.ca.gov/dataset/dayflow>

² Downloaded from: <https://apps.wildlife.ca.gov/FMWT>

Preliminary model comparison was performed using leave-one-out cross validation (LOO; Vehtari et al. 2017). Measures of model predictive accuracy using LOO are asymptotically equal to the widely applicable information criteria (WAIC; Watanabe 2010), but in the case of finite data LOO has been shown to be more robust to influential observations like outliers (Vehtari et al. 2017). The extent of model overlap in predictive accuracy was measured by the differences (and the standard errors of the differences) in expected log pointwise predictive densities, i.e., the differences in out-of-sample predictive accuracy between models. The preliminary model comparisons indicated there was a relatively high degree of similarity in terms of predictive ability between the top scoring individual models.

Therefore, rather than selecting a single model for inference, the posterior predictive probability distributions were combined as a weighted average across models. This process involved taking draws from the posterior of each single model in proportion to its model weight, with model weights for averaging posterior predictive distributions calculated using the *loo* package (Vehtari et al. 2020). For example, if a single model's weight was 25 percent of the total model set, then 2,500 draws from its posterior were added to the averaged posterior predictive distribution, which included 10,000 total draws taken across the posterior predictive distributions for all models. The statistical approach used to calculate the model weights for averaging the posterior predictive distributions across models is known as “stacking” (Yao et al. 2018).

Compared to more traditional model averaging approaches, stacking differs in terms of how model weights are assigned. Instead of calculating model weights based on the relative predictive ability for each individual model—where the best model for prediction would be given the highest weight—the model weights estimated through stacking minimize the LOO mean squared error of the resulting averaged posterior predictive distribution across models. In other words, stacking was used to estimate the optimal linear combination of model weights for averaging predictive distributions across the model set (Yao et al. 2018).

Hence, the model with the largest stacking weight does not necessarily have the highest predictive score compared to other models in the set. For example, the models in this case can be divided into two subsets: one subset includes a covariate for Delta outflow during December-May and the other model subset includes a covariate for March-May Delta outflow (Table J.1-1). Comparing the predictive ability of each individual model using LOO resulted in a model with December-May outflow (the model with the third highest stacking weight in Table J.1-1) having the highest individual predictive accuracy of any single model considered. In contrast, when the optimal linear combination of weighted model predictions was calculated, stacking resulted in a model with March-May Delta outflow having the highest single model weight (37 percent of the total stacking weight across the model set). Nevertheless, because stacking optimizes the linear combination of model weights for predictive accuracy, the next four models (~63 percent of the stacking weight) all include December-May Delta outflow instead of March-May Delta outflow. Therefore, in this case, even though the model with highest stacking weight included March-May Delta outflow, the averaged posterior predictive distribution was ultimately weighted more heavily with models that include December-May Delta outflow compared to models with March-May Delta outflow. Of the twelve models considered, the top five models by stacking weight accounted for >99.9 percent of the averaged posterior predictive distribution (Table J.1-1).

Predictions of the fall midwater trawl abundance index under the modeled CalSim 3 outflow scenarios (1922–2022) were generated using the model stacking approach described above to generate a weighted average Bayesian posterior predictive distribution across the set of models considered. Dropping subscripts denoting individual models for simplicity, the general form of the models can be written as:

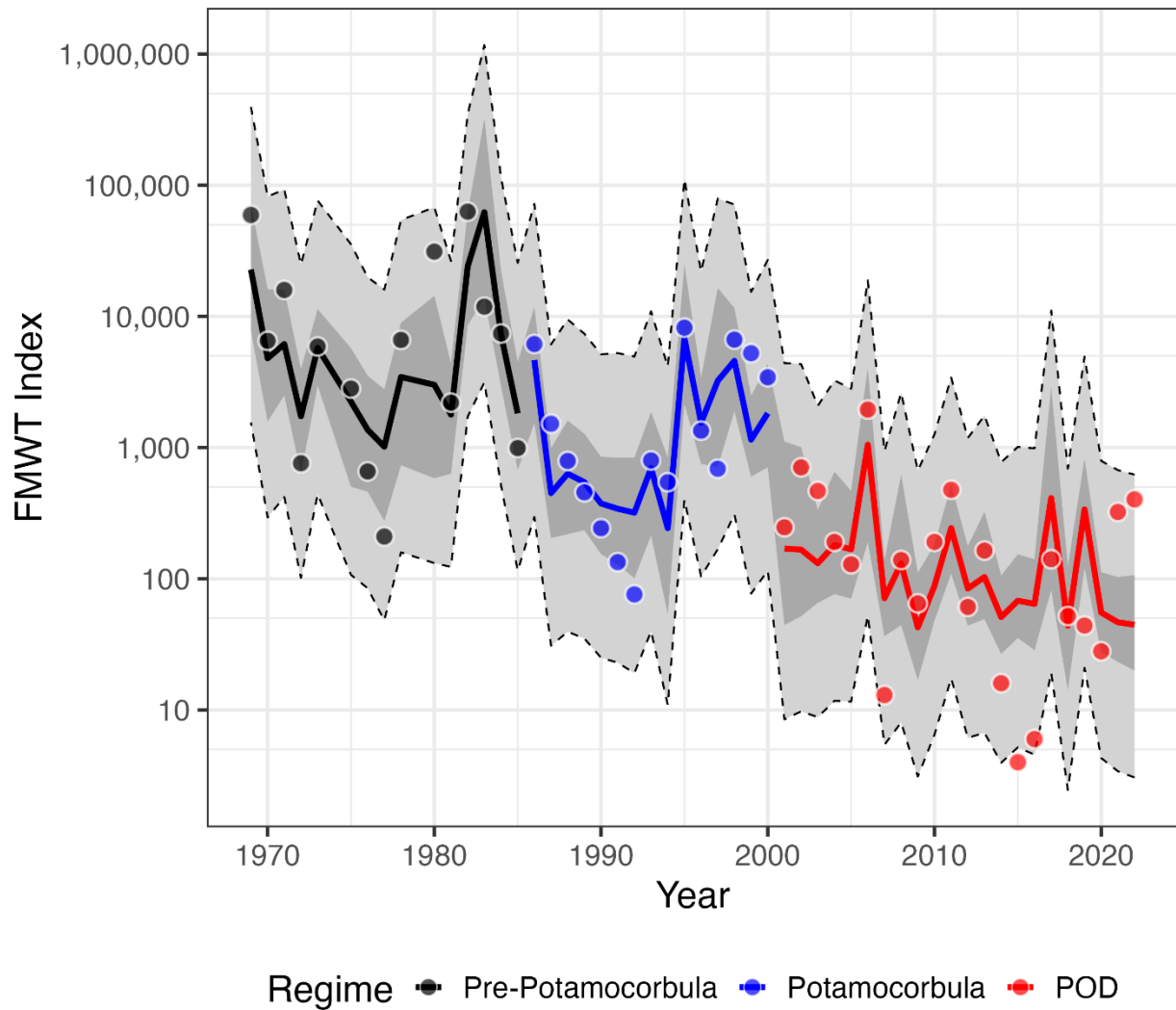
$$\text{Log}_{10}[\text{FMWT}_{yr}] \sim N(\mu_{yr}, \sigma^2) \quad (1)$$

$$\mu_{yr} = \beta_{0,i} + \beta_1 \text{Outflow}_{yr,j} + \beta_2 \text{Log}_{10}[\text{FMWT}_{yr-2}] + \beta_3 \text{Regime}_i * \text{Outflow}_{yr,j} \quad (2)$$

where:

- $\text{Log}_{10}[\text{FMWT}_{yr}]$ is the model predicted Log_{10} value of the fall midwater trawl index in water year yr ;
- μ_{yr} is the expected fall midwater trawl index in water year yr (the stacked posterior predictive distribution for μ_{yr} is shown as the dark grey ribbon in Figure J.1-1 Figure J.1-1);
- σ^2 is the residual variance parameter (the stacked posterior predictive distribution including the residual variance is shown as the light grey ribbon in Figure J.1-1 Figure J.1-1);
- $\beta_{0,i}$ represents the intercept parameter estimated for each regime: Pre-*Potamocorbula* ($i = 1$); *Potamocorbula* ($i = 2$); and POD ($i\beta_{0,i}^{\text{OBJ}}; \beta_{0,i}^{\text{OBJ}}$);
- β_1 represents the slope parameter estimated for the relationship between the fall midwater trawl index and Delta outflow;
- $\text{Outflow}_{yr,j}$ is the normalized³ outflow level during water year yr , and j denotes the outflow level during either the December through May, or the March through May period;
- β_2 represents the slope parameter estimated for the relationship between the expected fall midwater trawl index and the value of that index 2 years prior. For models without the parental stock covariate, $\beta_2 = 0$, and;
- β_3 represents the interaction covariate (the difference in slopes) with respect to the estimated effect of outflow on the FMWT index of abundance during different regimes (The asterisk “*” sign represents an interaction term between Regime and Delta Outflow). For models without this interaction term, $\beta_3 = 0$.

³ Normalized outflow values for each CalSim 3 scenario were calculated by subtracting the mean and dividing by the standard deviation of observed Delta outflow values (1967–2020).



Note: The circles represent the annual historical values of the fall midwater trawl abundance index. Colors correspond to the three modeled regimes. The solid lines connect the annual expected values from the stacked Bayesian posterior distribution. The darker gray ribbon represents the 95% posterior probability interval for the annual expected values for the fall midwater trawl index value. The lighter gray ribbon with a dashed black outline represents the averaged 95% overall posterior predictive probability interval for the fall midwater trawl index value. The posterior uncertainty interval (dark gray ribbon) has a smaller range than the posterior predictive interval (light gray ribbon) because in addition to uncertainty in the estimated model covariate values, the posterior predictive distribution also incorporates uncertainty in the residual error of the model fits (Equations 1 and 2 below).

Figure J.1-1. Stacked Posterior Predictive Distributions for the Log-Linear Regressions of Longfin Smelt Fall Midwater Trawl Abundance Index as a Function of Delta Outflow (December–May), Ecological Regime (1967–1987, pre-*Potamocorbula amurensis* invasion; 1988–2002, post-*Potamocorbula* invasion [shown as *Potamocorbula*]; and 2003–2022, Pelagic Organism Decline [POD]), and Abundance Index 2 Years Earlier [$\text{Log}_{10} \text{FMWT}(\text{yr} - 2)$].

For those models that included the Log_{10} FMWT($\text{yr} - 2$) parental stock size covariate (Table J.11 Table J.1-1), the starting parental stock size in 1922 and 1923 was set at a FMWT index value of 118.2, corresponding to the mean index value from 2013 through 2022. Given the starting values for the FMWT index (in the relevant models), the recursive nature of the regression formula was used to generate the expected FMWT index value in successive years from the posterior predictive distribution two years prior. For all models, predictions were conditional on the estimated relationship between the FMWT index and Delta outflow (in December–May, or March–May, depending on the model), and for those models that included a regime covariate, draws from the posterior predictive distributions were conditioned on estimates during the Pelagic Organism Decline regime.

Table J.111-1. The Optimal Linear Combination of Model Weights based on Stacking, which Minimizes the Mean Squared Error of the Leave-One-Out Cross Validation for the Resulting Model Averaged Posterior Predictive Distribution across the Twelve Log-Linear Regressions of Longfin Smelt Fall Midwater Trawl Abundance Index. Models are a Function of Delta Outflow (December–May or March–May), Ecological Regime (1967–1987, pre-*Potamocorbula amurensis* invasion; 1988–2002, post-*P. amurensis* invasion; and 2003–2022, Pelagic Organism Decline), and Abundance Index 2 Years Earlier (Log_{10} FMWT($\text{yr} - 2$)).

Log_{10}FMWT Linear Regression Model ^a	Stacking Weight
Mar–May + Regime + Log_{10} FMWT($\text{yr} - 2$)	0.3661
Dec–May + Regime + Log_{10} FMWT($\text{yr} - 2$)	0.2134
Dec–May + Regime + Dec–May*Regime	0.1636
Dec–May + Regime	0.1469
Dec–May + Log_{10} FMWT($\text{yr} - 2$)	0.1099
Mar–May + Regime + Mar–May*Regime + Log_{10} FMWT($\text{yr} - 2$)	<0.0001
Dec–May	<0.0001
Mar–May + Log_{10} FMWT($\text{yr} - 2$)	<0.0001
Dec–May + Regime + Dec–May*Regime + Log_{10} FMWT($\text{yr} - 2$)	<0.0001
Mar–May + Regime + Mar–May*Regime	<0.0001
Mar–May + Regime	<0.0001
Mar–May	<0.0001

^a An asterisk “*” sign represents an interaction term between Regime and Delta Outflow.

As an example, starting in 1924, draws from the posterior predictive distribution for models including the parental stock size covariate were generated by first substituting the normalized 1924 December through May (or March through May) CalSim 3 outflow value for each alternative. CalSim 3 outflow values prior to normalization (i.e., in units of million acre-feet) are shown in Figure J.1-2. Draws from the posterior distributions for the regression parameters and

the starting value for $\text{Log}_{10}[\text{FMWT}_{1922}]$ were then used to generate the posterior predictive distribution for the fall midwater trawl index in 1924 (μ_{1924}). This value was then substituted into Equation 1, and the posterior distribution for the residual variance parameter was used to generate draws from the pointwise posterior predictive distributions for the fall midwater trawl index.⁴ This process was iterated over each successive year, substituting the derived μ_{yr-2} values for $\text{Log}_{10}[\text{FMWT}_{yr-2}]$ to calculate μ_{yr} , and to generate the annual posterior predictive distributions for the fall midwater trawl index under each alternative. For models that did not include the parental stock size covariate, the posterior predictive distributions were generated based on the corresponding CalSim 3 outflow values for the monthly period corresponding to the individual model estimates, and likewise conditioned on covariate estimates during the POD regime for models that included a regime covariate (or the constant intercept parameter β_0 , for models without the regime covariate). As noted above in the description of the model stacking approach, draws from the posterior predictive distribution for each model were sampled in proportion to the stacking model weights, to generate a weighted average posterior predictive distribution across the models considered. Summaries were then calculated by grouping the stacked annual posterior predictive distributions by water year type and calculating the means and Bayesian credible intervals for each aggregated water year type posterior predictive distribution.

J.1.2.2 Assumptions / Uncertainty

Several additional models were also examined, in addition to those in Table J.11 Table J.1-1, but they were ultimately not included in this analysis due to poor model fits and what would have been additional computational cost without an expected difference in results (i.e., the poor model fits are indicative of poor model predictive accuracy, and hence tiny model weights). The additional models included a squared term on Delta outflow and their examination was motivated by the modeling results of Nobriga and Rosenfield (2016). Those authors assessed the relationship between Delta outflow and the ratio of age-0 to age-2 Longfin Smelt abundance in the two-life-stage versions of the models included in their analyses. They found support for non-linearity in this relationship (i.e., there was a peak in productivity at more intermediate outflow values), which led to the inclusion of a second-order polynomial regression (i.e., a squared term) on Delta outflow (Nobriga and Rosenfield 2016:50). Given the approach taken here, which differs from the Nobriga and Rosenfield analysis in terms of: (1) the survey data used for Longfin Smelt abundance; (2) how Delta outflow values were included as covariates, and; (3) the overall time periods for available data included in the regression models, there was little to no support found for a second-order polynomial regression on Delta outflow. The aforementioned factors that differed between the two analyses are briefly described in the next paragraph for completeness; but, given the poor predictive ability of the second-order polynomial regressions under the current approach, that subset of models was ultimately not included because the preliminary results indicated the stacked model weights would be near zero. Hence the averaged posterior predictive distributions would not be expected to be sensitive to the exclusion of those models in this case, but their inclusion would have increased the computational time necessary to run and perform the averaging over a larger set of models.

⁴ " $\sim N$ " in Eqn. 1 denotes a normal (Gaussian) distribution.

As outlined above, there are several differences between these analyses and those of Nobriga and Rosenfield (2016) that might explain the discrepancy in terms of support (or lack thereof) found for dome shaped Longfin Smelt productivity as a function of Delta outflow. Firstly, Nobriga and Rosenfield (2016) found support for this relationship fitting models to catch data from the San Francisco Bay Study. In these analyses, on the other hand, the regression models have been fit to the FMWT index of abundance instead. Second, Nobriga and Rosenfield (2016) incorporated covariate values for Delta Outflow based on a principal component analysis (the first principal component values) of the *z*-scored monthly means from December to May. Here, the monthly total outflows (either from December to May, or March to May) were summed, resulting in a total outflow value during each time period each year, and the regression covariate values were calculated as the *z*-scores of the period-total outflow values taken across years. Third, in addition to examining indices of abundance from different surveys, the annual time periods that have been examined also differ. Nobriga and Rosenfield (2016) examined the relationship between annual indices of Longfin Smelt abundance-at-age and Delta outflow that were available from the Bay Study during 1980–2013. In these analyses, this relationship was examined over a longer period (1967–2022), which includes >20 additional years in the comparison between Longfin Smelt abundance and Delta outflow.

This evaluation of management scenarios assumes that the correlation between outflow and the FMWT index of Longfin Smelt abundance during the POD regime (2003-2022) will remain constant in the future. While a positive correlation between outflow and the FMWT index has been evident for over 50 years of FMWT surveys, the strength of this relationship does not appear constant through time. For example, the results of Bayesian stacking indicates that averaging over models with ecological regime (at least as defined here) maximizes the out-of-sample predictive ability of models. In other words, these results indicate the FMWT data are consistent with shifts in stock productivity between regimes as a function of outflow. Only one model, with no regime covariate (equivalent to assuming the FMWT correlation with outflow has been constant since 1967) was assigned any substantial (~10%) weighting in the final averaged model set (Table J.1-1). In the absence of empirical data on whether or how this correlation may change in the future, it is reasonable to evaluate the management scenarios based on the correlation during the most recent ecological regime.

J.1.2.3 Code and Data Repository

Analysis files and code for the Longfin Smelt Outflow analysis are available upon request.

J.1.3 Results

Table J.11-22. Means of annual posterior predictive means for the FMWT index of Longfin Smelt abundance by water year type (WYT) for BA scenarios.

WYT	EXP1	EXP3	NAA	Alt2wTUCP woVA	Alt2woTUCP woVA	Alt2woTUCP DeltaVA	Alt2woTUCP AllVA
Wet	2186.2	1626.5	725.6	704.6	701.5	713.9	716.3
Above Normal	592.7	423.6	215.8	210.9	208.8	215.0	221.8

WYT	EXP1	EXP3	NAA	Alt2wTUCP woVA	Alt2woTUCP woVA	Alt2woTUCP DeltaVA	Alt2woTUCP AllVA
Below Normal	216.0	170.2	104.8	103.8	103.0	105.6	109.1
Dry	196.3	151.2	95.9	95.5	94.7	96.4	99.2
Critical	130.7	107.3	76.4	76.8	77.8	77.8	79.1

Table J.1-313. Means of annual posterior predictive means for the FMWT index of Longfin Smelt abundance by water year type (WYT) for EIS Scenarios. The percentage difference between scenarios and NAA is shown in the parentheses.

WYT	NAA	Alt1	Alt2 wTUCP woVA	Alt2 woTUCP woVA	Alt2 woTUCP DeltaVA	Alt2 woTUCP AllVA	Alt3	Alt4
Wet	725.6	664.2 (-8%)	711.7 (-2%)	709.3 (-2%)	717.2 (-1%)	727.1 (0%)	1015.7 (40%)	728.6 (0%)
Above Normal	215.8	194.0 (-10%)	210.8 (-2%)	209.4 (-3%)	214.9 (0%)	222.4 (3%)	285.4 (32%)	214.4 (-1%)
Below Normal	104.8	96.1 (-8%)	102.9 (-2%)	102.4 (-2%)	105.0 (0%)	108.7 (4%)	129.0 (23%)	104.4 (0%)
Dry	95.9	88.2 (-8%)	95.2 (-1%)	95.2 (-1%)	97.0 (1%)	99.9 (4%)	116.8 (22%)	95.3 (-1%)
Critical	76.4	72.3 (-5%)	75.9 (-1%)	77.5 (1%)	77.7 (2%)	79.6 (4%)	91.0 (19%)	75.6 (-1%)

Table J.1-414. Means of annual posterior predictive distributions for the FMWT index of Longfin Smelt abundance. Water year types (WYT) are shown by first initial (see Table J.11Table J.1-1 to reference full names for each type). The percentage difference between scenarios and NAA is shown in the parentheses.

Water Year	WYT	NAA	Alt1	Alt2 wTUCP woVA	Alt2 woTUCP woVA	Alt2 woTUCP DeltaVA	Alt2 woTUCP AllVA	Alt3	Alt4
1922	AN	121.2	113.9 (-6%)	117.2 (-3%)	116.9 (-4%)	120.7 (0%)	123.5 (2%)	142.4 (17%)	119.8 (-1%)
1923	BN	84.7	80.2 (-5%)	83.5 (-1%)	83.2 (-2%)	85.1 (1%)	87.1 (3%)	97.0 (15%)	83.1 (-2%)
1924	C	59.4	59.2 (0%)	59.2 (0%)	61.0 (3%)	61.8 (4%)	62.8 (6%)	64.6 (9%)	58.7 (-1%)
1925	D	84.4	80.2 (-5%)	85.4 (1%)	84.8 (0%)	86.8 (3%)	88.9 (5%)	99.8 (18%)	84.5 (0%)

Water Year	WYT	NAA	Alt1	Alt2 wTUCP woVA	Alt2 woTUCP woVA	Alt2 woTUCP DeltaVA	Alt2 woTUCP AllVA	Alt3	Alt4
1926	D	69.3	65.9 (-5%)	68.8 (-1%)	69.6 (0%)	70.0 (1%)	70.9 (2%)	74.4 (7%)	68.9 (-1%)
1927	W	193.1	167.5 (-13%)	197.5 (2%)	195.7 (1%)	199.2 (3%)	207.1 (7%)	250.0 (29%)	197.2 (2%)
1928	AN	111.2	101.4 (-9%)	109.1 (-2%)	109.0 (-2%)	112.6 (1%)	116.6 (5%)	130.7 (18%)	113.9 (2%)
1929	C	70	67.0 (-4%)	70.2 (0%)	71.7 (2%)	72.0 (3%)	73.9 (6%)	85.3 (22%)	69.4 (-1%)
1930	D	77.9	69.6 (-11%)	78.2 (0%)	77.4 (-1%)	79.3 (2%)	81.1 (4%)	90.8 (16%)	79.2 (2%)
1931	C	54	53.5 (-1%)	53.8 (0%)	55.4 (3%)	56.1 (4%)	57.4 (6%)	59.6 (10%)	53.7 (-1%)
1932	C	67.9	62.2 (-8%)	67.2 (-1%)	69.3 (2%)	70.1 (3%)	71.2 (5%)	79.9 (18%)	67.9 (0%)
1933	C	51.1	50.4 (-2%)	50.8 (-1%)	52.7 (3%)	53.2 (4%)	54.0 (6%)	53.9 (5%)	50.6 (-1%)
1934	C	55.4	54.2 (-2%)	55.0 (-1%)	57.5 (4%)	57.5 (4%)	58.3 (5%)	60.7 (9%)	55.2 (0%)
1935	BN	80.4	74.4 (-7%)	81.2 (1%)	80.2 (0%)	80.4 (0%)	82.8 (3%)	89.1 (11%)	81.2 (1%)
1936	BN	106	94.7 (-11%)	102.9 (-3%)	102.7 (-3%)	102.7 (-3%)	107.1 (1%)	110.4 (4%)	104.0 (-2%)
1937	BN	91.4	83.6 (-8%)	88.8 (-3%)	88.7 (-3%)	90.4 (-1%)	92.5 (1%)	102.3 (12%)	88.7 (-3%)
1938	W	794.6	749.8 (-6%)	770.9 (-3%)	770.8 (-3%)	770.6 (-3%)	777.3 (-2%)	1123.6 (41%)	778.3 (-2%)
1939	D	59.5	56.3 (-5%)	59.2 (0%)	59.1 (-1%)	59.8 (1%)	60.7 (2%)	66.0 (11%)	58.7 (-1%)
1940	AN	404.1	369.0 (-9%)	391.5 (-3%)	394.4 (-2%)	391.6 (-3%)	413.1 (2%)	528.9 (31%)	400.7 (-1%)
1941	W	364.9	336.3 (-8%)	352.9 (-3%)	351.9 (-4%)	353.9 (-3%)	353.3 (-3%)	424.8 (16%)	365.8 (0%)
1942	W	570.1	511.7 (-10%)	556.4 (-2%)	569.1 (0%)	564.0 (-1%)	581.6 (2%)	791.6 (39%)	580.6 (2%)
1943	W	283.5	258.6 (-9%)	273.1 (-4%)	269.8 (-5%)	279.8 (-1%)	283.9 (0%)	385.1 (36%)	283.3 (0%)
1944	D	138.1	126.2 (-9%)	134.4 (-3%)	137.2 (-1%)	137.5 (0%)	143.0 (4%)	171.3 (24%)	136.1 (-1%)

Water Year	WYT	NAA	Alt1	Alt2 wTUCP woVA	Alt2 woTUCP woVA	Alt2 woTUCP DeltaVA	Alt2 woTUCP AIIVA	Alt3	Alt4
1945	D	126.3	112.3 (-11%)	124.7 (-1%)	123.4 (-2%)	127.4 (1%)	131.7 (4%)	162.3 (29%)	125.9 (0%)
1946	BN	144.1	126.1 (-12%)	141.2 (-2%)	142.1 (-1%)	146.2 (1%)	152.8 (6%)	182.1 (26%)	141.5 (-2%)
1947	D	73.4	69.7 (-5%)	73.5 (0%)	73.2 (0%)	74.3 (1%)	75.6 (3%)	87.6 (19%)	73.4 (0%)
1948	D	89.4	85.7 (-4%)	89.4 (0%)	89.5 (0%)	91.6 (2%)	94.9 (6%)	107.8 (21%)	88.1 (-1%)
1949	D	74.4	69.8 (-6%)	74.6 (0%)	74.4 (0%)	75.2 (1%)	77.8 (5%)	80.2 (8%)	74.1 (0%)
1950	D	80.7	74.6 (-7%)	80.3 (0%)	80.5 (0%)	82.8 (3%)	86.5 (7%)	91.1 (13%)	79.8 (-1%)
1951	AN	172	156.4 (-9%)	167.9 (-2%)	168.3 (-2%)	174.0 (1%)	176.6 (3%)	200.0 (16%)	169.6 (-1%)
1952	W	331.7	296.4 (-11%)	319.1 (-4%)	318.7 (-4%)	324.1 (-2%)	330.5 (0%)	421.0 (27%)	329.4 (-1%)
1953	AN	142.9	128.5 (-10%)	140.3 (-2%)	141.2 (-1%)	146.1 (2%)	150.7 (5%)	177.8 (24%)	143.5 (0%)
1954	AN	149.9	128.3 (-14%)	143.7 (-4%)	143.4 (-4%)	147.2 (-2%)	154.1 (3%)	203.0 (35%)	148.3 (-1%)
1955	D	76.5	70.9 (-7%)	75.6 (-1%)	75.8 (-1%)	78.0 (2%)	79.6 (4%)	96.6 (26%)	76.5 (0%)
1956	W	522.6	464.0 (-11%)	504.2 (-4%)	506.8 (-3%)	515.6 (-1%)	530.0 (1%)	727.4 (39%)	526.5 (1%)
1957	BN	80.1	73.5 (-8%)	78.6 (-2%)	78.6 (-2%)	81.0 (1%)	84.3 (5%)	100.1 (25%)	79.0 (-1%)
1958	W	1085	911.6 (-16%)	1045.5 (-4%)	1048.2 (-3%)	1061.7 (-2%)	1084.5 (0%)	1613.1 (49%)	1074.1 (-1%)
1959	BN	74.8	70.0 (-6%)	74.0 (-1%)	73.8 (-1%)	75.8 (1%)	78.3 (5%)	90.7 (21%)	74.6 (0%)
1960	D	188.6	172.5 (-9%)	186.7 (-1%)	190.5 (1%)	191.2 (1%)	199.6 (6%)	262.0 (39%)	185.8 (-1%)
1961	D	63.2	57.8 (-9%)	63.0 (0%)	62.8 (-1%)	64.0 (1%)	65.1 (3%)	70.8 (12%)	62.3 (-1%)
1962	D	118.9	109.2 (-8%)	117.4 (-1%)	118.1 (-1%)	121.9 (3%)	127.1 (7%)	156.8 (32%)	117.9 (-1%)
1963	W	147.3	128.5 (-13%)	145.6 (-1%)	145.3 (-1%)	149.0 (1%)	152.4 (3%)	173.8 (18%)	146.0 (-1%)

Water Year	WYT	NAA	Alt1	Alt2 wTUCP woVA	Alt2 woTUCP woVA	Alt2 woTUCP DeltaVA	Alt2 woTUCP AIIVA	Alt3	Alt4
1964	D	71	67.6 (-5%)	70.5 (-1%)	70.8 (0%)	72.8 (3%)	74.2 (4%)	88.0 (24%)	71.2 (0%)
1965	W	238.2	205.1 (-14%)	235.2 (-1%)	234.0 (-2%)	241.2 (1%)	243.9 (2%)	321.3 (35%)	237.9 (0%)
1966	BN	72.5	66.1 (-9%)	71.3 (-2%)	71.6 (-1%)	73.5 (1%)	75.8 (5%)	89.7 (24%)	72.7 (0%)
1967	W	279.5	234.8 (-16%)	271.7 (-3%)	272.3 (-3%)	280.2 (0%)	289.9 (4%)	392.5 (40%)	277.7 (-1%)
1968	BN	79.2	73.6 (-7%)	79.1 (0%)	79.2 (0%)	81.5 (3%)	83.7 (6%)	93.5 (18%)	82.0 (4%)
1969	W	719.9	640.2 (-11%)	717.0 (0%)	714.5 (-1%)	719.6 (0%)	737.7 (2%)	1091.5 (52%)	724.7 (1%)
1970	W	288.5	280.2 (-3%)	280.8 (-3%)	281.2 (-3%)	288.4 (0%)	289.9 (0%)	381.6 (32%)	296.1 (3%)
1971	W	301.7	263.9 (-13%)	301.8 (0%)	296.9 (-2%)	300.2 (0%)	310.5 (3%)	460.4 (53%)	305.2 (1%)
1972	BN	97.4	87.1 (-11%)	93.7 (-4%)	93.7 (-4%)	98.2 (1%)	101.1 (4%)	128.9 (32%)	98.3 (1%)
1973	AN	303.5	259.6 (-14%)	297.2 (-2%)	296.9 (-2%)	307.8 (1%)	322.4 (6%)	436.0 (44%)	306.0 (1%)
1974	W	476.1	412.3 (-13%)	464.1 (-3%)	467.5 (-2%)	472.0 (-1%)	477.4 (0%)	623.7 (31%)	477.6 (0%)
1975	AN	223	189.3 (-15%)	215.6 (-3%)	212.2 (-5%)	224.6 (1%)	230.5 (3%)	313.0 (40%)	222.1 (0%)
1976	C	97.3	90.9 (-7%)	95.1 (-2%)	96.3 (-1%)	96.0 (-1%)	98.1 (1%)	119.6 (23%)	96.8 (-1%)
1977	C	76.1	73.4 (-4%)	75.5 (-1%)	76.5 (1%)	78.7 (3%)	80.3 (6%)	89.5 (18%)	76.3 (0%)
1978	AN	182	167.2 (-8%)	182.4 (0%)	179.4 (-1%)	182.7 (0%)	188.2 (3%)	259.7 (43%)	180.8 (-1%)
1979	D	81.1	74.2 (-9%)	79.0 (-3%)	78.9 (-3%)	81.8 (1%)	84.4 (4%)	95.4 (18%)	79.9 (-1%)
1980	AN	316.5	295.4 (-7%)	308.7 (-2%)	310.0 (-2%)	319.2 (1%)	334.1 (6%)	415.2 (31%)	303.7 (-4%)
1981	D	66.8	62.4 (-7%)	65.9 (-1%)	65.7 (-2%)	67.9 (2%)	70.0 (5%)	77.2 (16%)	67.3 (1%)
1982	W	1151	1015.8 (-12%)	1120.3 (-3%)	1121.0 (-3%)	1126.7 (-2%)	1162.5 (1%)	1599.6 (39%)	1124.3 (-2%)

Water Year	WYT	NAA	Alt1	Alt2 wTUCP woVA	Alt2 woTUCP woVA	Alt2 woTUCP DeltaVA	Alt2 woTUCP AIIVA	Alt3	Alt4
1983	W	3476.1	3336.9 (-4%)	3475.2 (0%)	3430.3 (-1%)	3527.1 (1%)	3516.7 (1%)	4489.4 (29%)	3577.9 (3%)
1984	W	676.6	593.1 (-12%)	654.9 (-3%)	656.8 (-3%)	661.3 (-2%)	684.2 (1%)	962.2 (42%)	643.5 (-5%)
1985	BN	229.3	212.9 (-7%)	222.6 (-3%)	221.2 (-4%)	225.0 (-2%)	234.5 (2%)	288.1 (26%)	223.4 (-3%)
1986	W	939.5	822.2 (-12%)	902.4 (-4%)	902.9 (-4%)	915.9 (-3%)	940.3 (0%)	1494.5 (59%)	900.7 (-4%)
1987	D	100.3	93.5 (-7%)	103.2 (3%)	102.4 (2%)	103.3 (3%)	106.2 (6%)	113.0 (13%)	101.5 (1%)
1988	C	168.9	143.8 (-15%)	162.8 (-4%)	164.3 (-3%)	159.1 (-6%)	171.1 (1%)	229.0 (36%)	161.3 (-4%)
1989	D	86.9	82.1 (-6%)	87.8 (1%)	87.2 (0%)	89.3 (3%)	91.1 (5%)	97.9 (13%)	87.7 (1%)
1990	C	79.1	74.3 (-6%)	80.7 (2%)	81.1 (2%)	80.4 (2%)	83.1 (5%)	95.0 (20%)	79.5 (0%)
1991	C	66.6	65.4 (-2%)	66.6 (0%)	67.7 (2%)	67.2 (1%)	70.7 (6%)	72.5 (9%)	66.6 (0%)
1992	C	66.9	64.4 (-4%)	69.1 (3%)	70.4 (5%)	70.6 (5%)	70.3 (5%)	74.5 (11%)	68.5 (2%)
1993	AN	148	124.0 (-16%)	145.0 (-2%)	135.5 (-8%)	137.6 (-7%)	138.4 (-7%)	183.4 (24%)	142.9 (-3%)
1994	C	57.1	55.2 (-3%)	57.6 (1%)	57.6 (1%)	58.2 (2%)	59.1 (3%)	62.3 (9%)	57.3 (0%)
1995	W	908.8	822.6 (-9%)	910.6 (0%)	896.9 (-1%)	877.5 (-3%)	898.1 (-1%)	1220.0 (34%)	925.9 (2%)
1996	W	220.8	215.8 (-2%)	212.0 (-4%)	210.4 (-5%)	213.3 (-3%)	213.1 (-3%)	275.8 (25%)	218.7 (-1%)
1997	W	1238.4	1133.0 (-9%)	1192.7 (-4%)	1194.4 (-4%)	1167.6 (-6%)	1203.2 (-3%)	1701.7 (37%)	1262.9 (2%)
1998	W	1026	1089.7 (6%)	1013.2 (-1%)	1009.8 (-2%)	1021.8 (0%)	1013.9 (-1%)	1339.3 (31%)	1065.3 (4%)
1999	W	586	519.6 (-11%)	553.3 (-6%)	559.3 (-5%)	546.2 (-7%)	562.1 (-4%)	856.0 (46%)	569.4 (-3%)
2000	AN	428.9	403.6 (-6%)	417.7 (-3%)	413.6 (-4%)	424.1 (-1%)	435.3 (1%)	590.0 (38%)	428.1 (0%)
2001	D	145.3	129.0 (-11%)	140.6 (-3%)	141.9 (-2%)	143.1 (-2%)	145.4 (0%)	178.9 (23%)	142.3 (-2%)

Water Year	WYT	NAA	Alt1	Alt2 wTUCP woVA	Alt2 woTUCP woVA	Alt2 woTUCP DeltaVA	Alt2 woTUCP AIIVA	Alt3	Alt4
2002	BN	161.2	151.1 (-6%)	158.5 (-2%)	155.7 (-3%)	160.3 (-1%)	169.1 (5%)	219.2 (36%)	160.8 (0%)
2003	AN	154.5	132.9 (-14%)	152.1 (-2%)	152.4 (-1%)	155.3 (1%)	158.1 (2%)	198.6 (29%)	153.6 (-1%)
2004	AN	164.1	146.0 (-11%)	162.7 (-1%)	158.9 (-3%)	165.8 (1%)	173.6 (6%)	217.0 (32%)	169.8 (3%)
2005	BN	147.2	129.2 (-12%)	142.4 (-3%)	141.4 (-4%)	146.1 (-1%)	150.4 (2%)	194.6 (32%)	146.0 (-1%)
2006	W	1352.3	1250.2 (-8%)	1347.4 (0%)	1321.8 (-2%)	1355.4 (0%)	1384.8 (2%)	2041.8 (51%)	1385.7 (2%)
2007	BN	79.3	72.4 (-9%)	77.4 (-2%)	76.9 (-3%)	79.2 (0%)	81.3 (2%)	98.0 (23%)	78.9 (-1%)
2008	D	190.4	168.1 (-12%)	189.0 (-1%)	186.5 (-2%)	188.3 (-1%)	194.4 (2%)	253.6 (33%)	187.1 (-2%)
2009	D	70.3	64.7 (-8%)	69.5 (-1%)	69.2 (-2%)	71.5 (2%)	74.8 (6%)	79.5 (13%)	70.4 (0%)
2010	BN	118.5	105.5 (-11%)	117.3 (-1%)	117.4 (-1%)	120.8 (2%)	125.3 (6%)	155.6 (31%)	118.3 (0%)
2011	W	289.7	263.6 (-9%)	279.7 (-3%)	278.3 (-4%)	284.3 (-2%)	287.1 (-1%)	394.8 (36%)	281.8 (-3%)
2012	BN	79.6	76.4 (-4%)	78.6 (-1%)	78.8 (-1%)	80.6 (1%)	83.1 (4%)	98.8 (24%)	82.3 (3%)
2013	D	108.8	97.5 (-10%)	106.9 (-2%)	106.6 (-2%)	108.8 (0%)	112.2 (3%)	132.7 (22%)	107.7 (-1%)
2014	C	58.5	57.0 (-3%)	57.9 (-1%)	58.5 (0%)	59.3 (1%)	59.6 (2%)	64.0 (9%)	58.1 (-1%)
2015	C	69.8	68.6 (-2%)	69.3 (-1%)	72.4 (4%)	73.1 (5%)	74.1 (6%)	81.7 (17%)	69.5 (0%)
2016	BN	83.9	78.3 (-7%)	83.5 (0%)	81.6 (-3%)	83.7 (0%)	87.0 (4%)	95.6 (14%)	84.6 (1%)
2017	W	1169.2	1077.1 (-8%)	1150.7 (-2%)	1155.7 (-1%)	1155.7 (-1%)	1144.7 (-2%)	1762.8 (51%)	1170.0 (0%)
2018	BN	77.1	74.6 (-3%)	77.5 (0%)	76.2 (-1%)	78.6 (2%)	81.2 (5%)	87.7 (14%)	79.4 (3%)
2019	W	684.8	596.1 (-13%)	667.4 (-3%)	673.9 (-2%)	694.2 (1%)	695.9 (2%)	1120.3 (64%)	657.9 (-4%)
2020	D	60.5	57.8 (-5%)	60.5 (0%)	59.9 (-1%)	61.2 (1%)	62.7 (4%)	69.4 (15%)	61.1 (1%)

Water Year	WYT	NAA	Alt1	Alt2 wTUCP woVA	Alt2 woTUCP woVA	Alt2 woTUCP DeltaVA	Alt2 woTUCP AIIVA	Alt3	Alt4
2021	C	124.6	117.2 (-6%)	123.9 (-1%)	126.2 (1%)	129.3 (4%)	130.1 (4%)	164.2 (32%)	120.5 (-3%)

Table J.1-5. 15Means of annual posterior predictive distributions for the FMWT index of Longfin Smelt abundance. Scenarios considered in the BA are shown for comparison across years.

Water Year	WYT	EXP1	EXP3	NAA	Alt2v1 wTUCP	Alt2v1 woTUCP	Alt2v2 woTUCP	Alt2v3 woTUCP
1922	Above Normal	221.4	158.2	121.2	117	116.5	119.8	122.4
1923	Below Normal	126.9	110.5	84.7	83.3	82.9	84.4	86.2
1924	Critical	74.7	70	59.4	59.4	61.2	61.5	62.6
1925	Dry	166	108.7	84.4	85.4	84.9	86.1	88.8
1926	Dry	101.1	86.2	69.3	69.7	70.3	70.4	72.4
1927	Wet	425.5	291.7	193.1	198.5	196.5	198.4	205.4
1928	Above Normal	199	168	111.2	110	109.6	112.4	117.2
1929	Critical	119.3	93.4	70	72.1	72.9	72.3	74.3
1930	Dry	150.6	108.2	77.9	77.4	77.3	78.6	81.4
1931	Critical	70	63.8	54	54.2	56.3	55.7	56.9
1932	Critical	137.4	89.8	67.9	66.8	69	69.2	70.5
1933	Critical	69.8	61.4	51.1	50.6	53.1	52.6	53.5
1934	Critical	89	68.7	55.4	55.3	57.3	57.3	58.1
1935	Below Normal	158.5	104.8	80.4	80.6	79.6	80.1	81.9
1936	Below Normal	228.1	158.1	106	103	102.8	103.1	106.9
1937	Below Normal	204.2	136.2	91.4	88.5	88.5	90.2	91.6
1938	Wet	2479.4	1760.3	794.6	762	763	773.2	765.2
1939	Dry	87.8	76.8	59.5	58.5	58.6	58.9	59.5
1940	Above Normal	1478.4	848.9	404.1	391.8	390	397.6	406.7
1941	Wet	967.2	722.3	364.9	346.2	346.1	346.9	343.4
1942	Wet	2033.6	1388.5	570.1	559.9	550.9	560.9	559.8
1943	Wet	790.9	616.5	283.5	270.5	268.6	274.7	282.4
1944	Dry	333.6	247.8	138.1	135.8	136.3	139	142.4
1945	Dry	336.4	247.7	126.3	122.8	122.4	125.9	129.7
1946	Below Normal	334.6	262	144.1	142.6	141.5	147.9	152
1947	Dry	138.2	110.1	73.4	73.5	72.3	72.8	75.2

Water Year	WYT	EXP1	EXP3	NAA	Alt2v1 wTUCP	Alt2v1 woTUCP	Alt2v2 woTUCP	Alt2v3 woTUCP
1948	Dry	199.5	143.8	89.4	91.5	90.6	93.2	95.2
1949	Dry	124.1	102.9	74.4	74.8	73.2	74	77
1950	Dry	163.5	114.3	80.7	80.6	80.8	82.6	84.9
1951	Above Normal	349.3	297.8	172	169.6	168.3	174	175.8
1952	Wet	966.9	653.5	331.7	319.6	319.7	321.9	322.3
1953	Above Normal	302.5	245.1	142.9	139.5	139	144.8	148.6
1954	Above Normal	366.9	270.3	149.9	145.6	145	148.7	154.1
1955	Dry	135.2	114.8	76.5	75.5	75.2	77.1	78.8
1956	Wet	1895.4	1254.1	522.6	509.1	509.4	522.1	529.7
1957	Below Normal	146.6	122.7	80.1	78.9	78.6	80.8	83.7
1958	Wet	3824.4	2821.6	1085	1040.7	1036.3	1054.9	1065.5
1959	Below Normal	118.2	109.5	74.8	73.1	72.6	75.1	76.4
1960	Dry	531.4	371.9	188.6	192	184	188.8	194.9
1961	Dry	99	83.4	63.2	62.7	62.4	63.3	64.1
1962	Dry	287	205.1	118.9	118.7	116.9	118.4	124.2
1963	Wet	268.8	219.8	147.3	145.3	144.6	146.9	150.1
1964	Dry	118.8	105.5	71	70.9	70.1	70.6	72.3
1965	Wet	611.4	420.1	238.2	236	232.3	236.5	243.6
1966	Below Normal	119.6	108.2	72.5	71.7	71.2	72.3	74.6
1967	Wet	858.8	599.7	279.5	273.5	270.1	277.8	288.2
1968	Below Normal	124.4	116	79.2	79.5	78.5	80	82.5
1969	Wet	2848.3	1885.7	719.9	735.9	725.1	721.8	731.1
1970	Wet	539.6	527.2	288.5	282.5	281.6	286.9	288.3
1971	Wet	1018.5	694.5	301.7	304.5	301.6	298.6	301.5
1972	Below Normal	180.6	162.4	97.4	96.3	96.2	97.9	100.7
1973	Above Normal	856.3	639.1	303.5	300.8	295	305.3	318.9
1974	Wet	988.9	892	476.1	466.7	464.6	469.8	469.4
1975	Above Normal	600.9	466.9	223	216.4	213.9	224.3	233
1976	Critical	154.4	155.3	97.3	96.5	96.4	96.3	98.6
1977	Critical	110.3	104.4	76.1	77.6	77.8	78.2	79.6
1978	Above Normal	569.3	329.6	182	182.8	178.3	184.9	189.4
1979	Dry	156	128.6	81.1	79.8	79.8	81.4	83.7
1980	Above Normal	946.4	666.4	316.5	308.3	303.8	316.7	331.2
1981	Dry	113.8	95.9	66.8	66.5	65.9	68.2	68.7
1982	Wet	3937.1	3016.6	1151	1099.6	1096.4	1110.1	1145.7
1983	Wet	7315.3	6540	3476.1	3375	3399.6	3507.9	3456.5

Water Year	WYT	EXP1	EXP3	NAA	Alt2v1 wTUCP	Alt2v1 woTUCP	Alt2v2 woTUCP	Alt2v3 woTUCP
1984	Wet	1969.9	1640.3	676.6	661	637.3	652.6	665.9
1985	Below Normal	432.7	407.5	229.3	226.7	226.4	231.3	238.6
1986	Wet	3519.7	2654.4	939.5	914.3	900.7	905.9	920.5
1987	Dry	159.4	143.1	100.3	102.2	102.2	101.6	104.9
1988	Critical	396.9	296.5	168.9	169.7	167.6	166.5	170.3
1989	Dry	163	126.4	86.9	87.5	87.2	88.2	90.2
1990	Critical	131.2	107.3	79.1	80.4	80.2	79.6	81.6
1991	Critical	99.4	80.6	66.6	66.6	68.5	66.7	67.5
1992	Critical	102	83.3	66.9	68.7	69.2	69.5	70.2
1993	Above Normal	366.8	224.9	148	140.7	130.3	135.1	137.1
1994	Critical	76.2	72.5	57.1	57.4	57.2	58	58.8
1995	Wet	3207.1	1785.3	908.8	887.8	865.6	877.7	885.7
1996	Wet	444.3	370.1	220.8	209.8	209.6	212	212.3
1997	Wet	4213.5	3145.6	1238.4	1162.7	1161.2	1170	1170.4
1998	Wet	3211.5	2402.7	1026	981.7	1002.8	1022.2	1013.9
1999	Wet	1729	1363	586	544.4	543.6	547.2	556.5
2000	Above Normal	1316.6	1041.4	428.9	415.3	422.1	427.5	438.1
2001	Dry	299.1	249.4	145.3	141.2	140.3	143	146.8
2002	Below Normal	407.4	310.8	161.2	159.8	159.9	163.6	173.1
2003	Above Normal	360.7	268.8	154.5	152.3	149.8	153.3	158.3
2004	Above Normal	363.7	305.4	164.1	162	161.1	165.1	174.3
2005	Below Normal	433.7	298.5	147.2	145.2	143.4	148.4	153.2
2006	Wet	3912.4	3117.8	1352.3	1316.3	1319.7	1371.1	1388
2007	Below Normal	150.3	125.3	79.3	78.5	77.3	80.1	81.7
2008	Dry	417.5	308.4	190.4	188	185.7	190.5	197.3
2009	Dry	134.1	97.3	70.3	69.7	68.8	71.3	74.2
2010	Below Normal	271.4	196.2	118.5	119.6	118	122.6	128.3
2011	Wet	687.3	536.4	289.7	278	277	280	283
2012	Below Normal	142.5	117.8	79.6	80.4	79	81.1	83.9
2013	Dry	204.2	170.9	108.8	107.1	107.3	108.3	111.5
2014	Critical	80.8	71.1	58.5	58.6	58.8	59.6	59.5
2015	Critical	116.9	95.1	69.8	69.8	72.7	73.3	73.5
2016	Below Normal	171.2	105.7	83.9	83.5	81.6	83.1	87.6
2017	Wet	3890.3	2596	1169.2	1155.3	1139.6	1141	1123.8
2018	Below Normal	137.5	111.1	77.1	76.3	76.4	77.8	80.8
2019	Wet	2657.9	1626.7	684.8	693.1	680	699.5	689.7

Water Year	WYT	EXP1	EXP3	NAA	Alt2v1 wTUCP	Alt2v1 woTUCP	Alt2v2 woTUCP	Alt2v3 woTUCP
2020	Dry	91.7	81.5	60.5	59.6	59.6	60.6	61.8
2021	Critical	262	203.7	124.6	124.8	125.9	128.2	130.6

Table J.1-61. The percentages of each water year type are shown for: (1) the CalSim 3 scenarios, and; (2) the historical water year types during 2003-2022 (POD regime).

	Wet	Above Normal	Below Normal	Dry	Critical
CalSim 3	28%	14%	18%	24%	16%
2003-2022 (POD regime)	25%	20%	25%	10%	20%

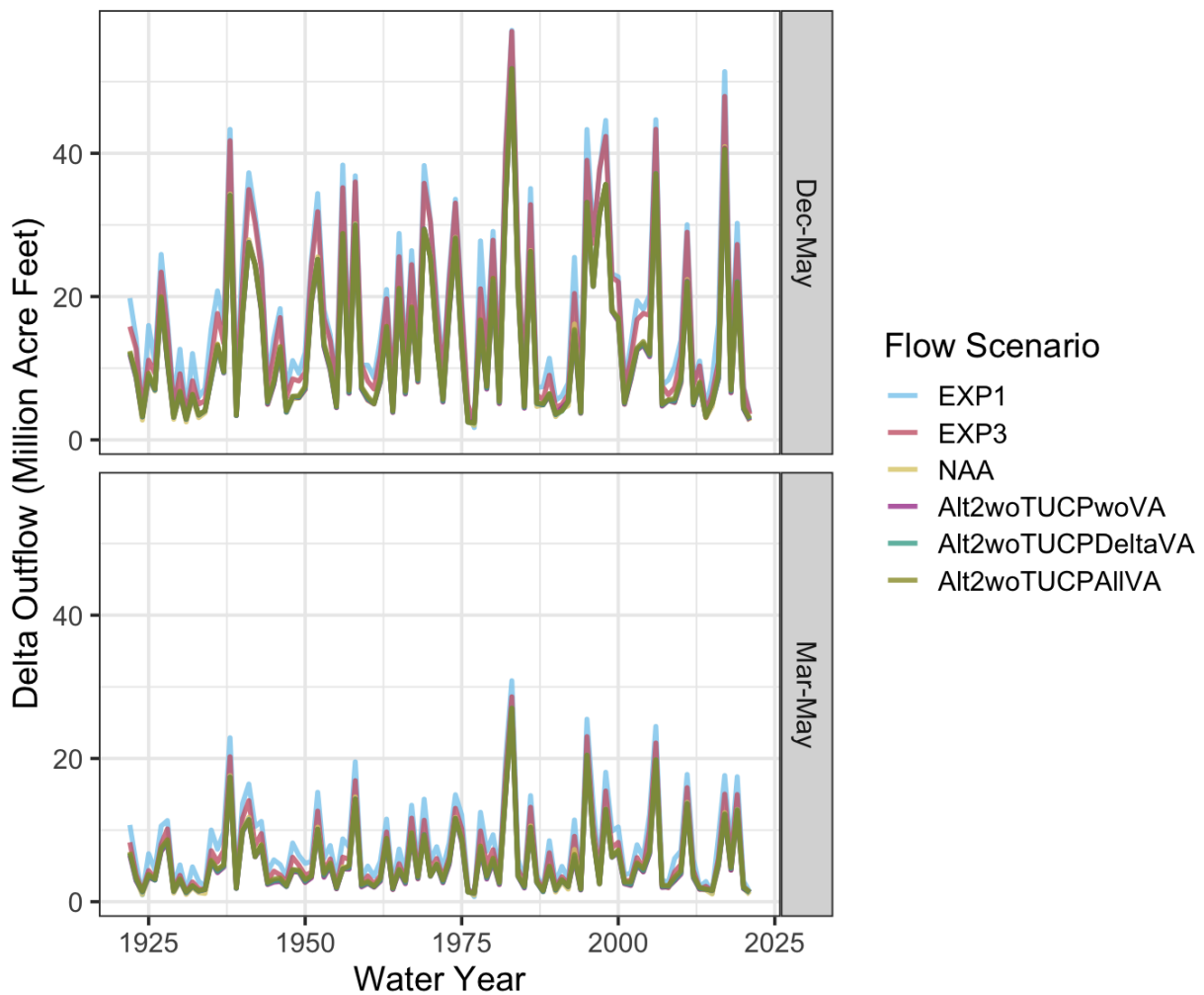


Figure J.1-212. CalSim 3 outflow values are shown for comparison across BA scenarios.

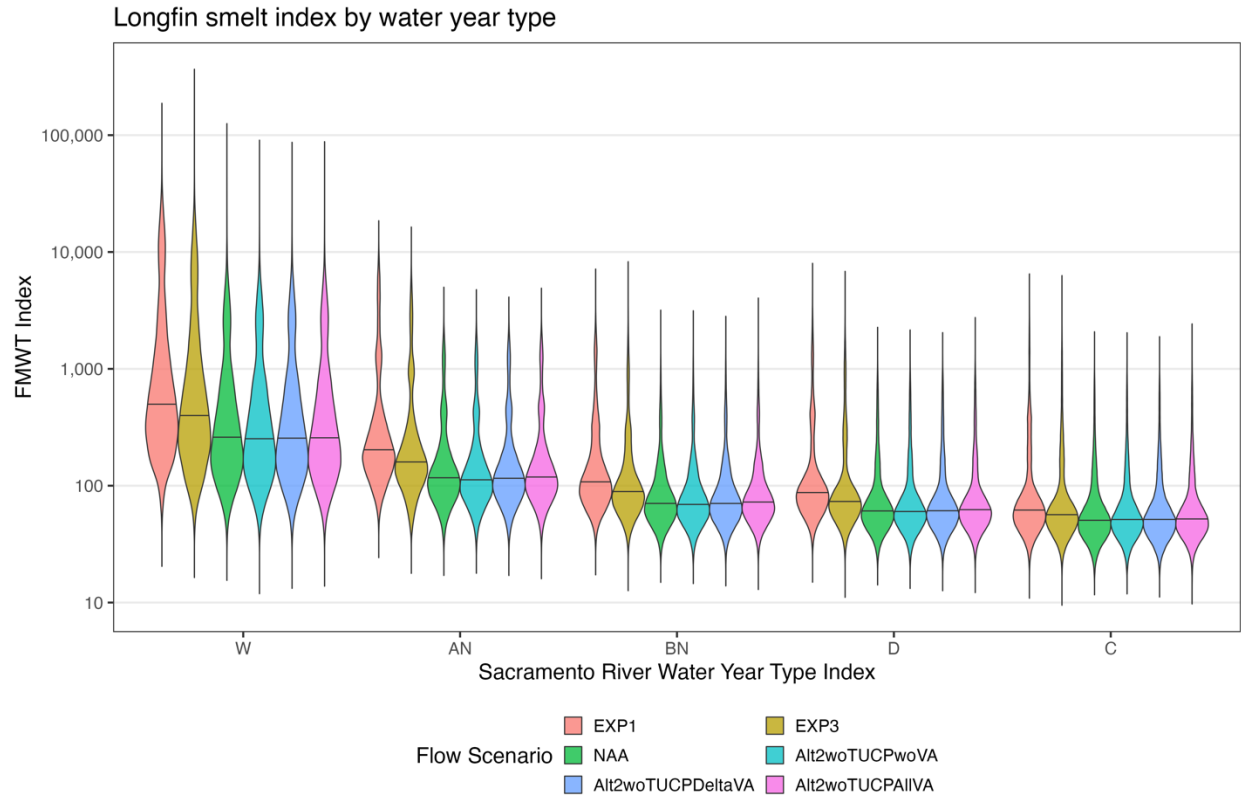


Figure J.1-3. Posterior predictive distributions for the FMWT index of Longfin Smelt abundance are shown aggregated by water year type⁵ for each BA scenario. The horizontal line in the distribution for each scenario represents the median predicted value.

⁵ <https://cdec.water.ca.gov/reportapp/javareports?name=WSIHIST>

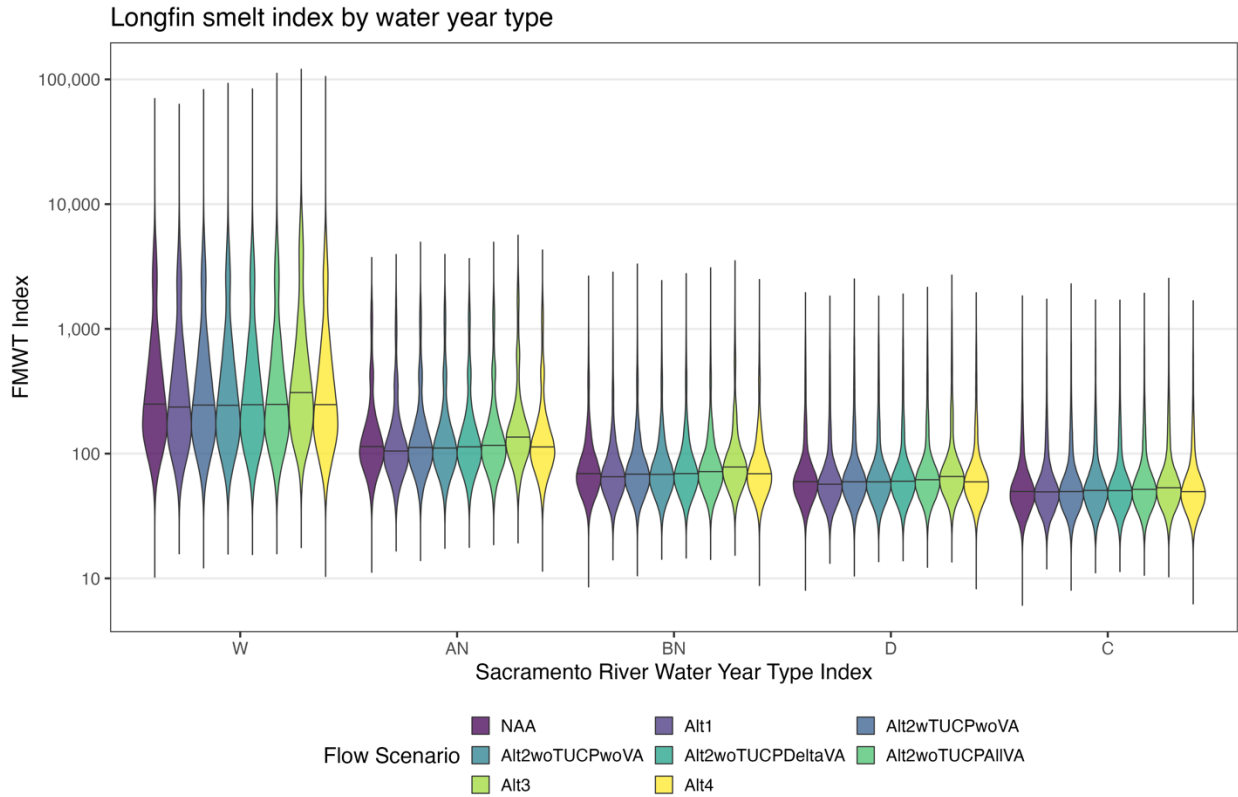


Figure J.1-4. Posterior predictive distributions for the FMWT index of Longfin Smelt abundance are shown aggregated by water year type for each EIS scenario. The horizontal line in the distribution for each scenario represents the median predicted value.

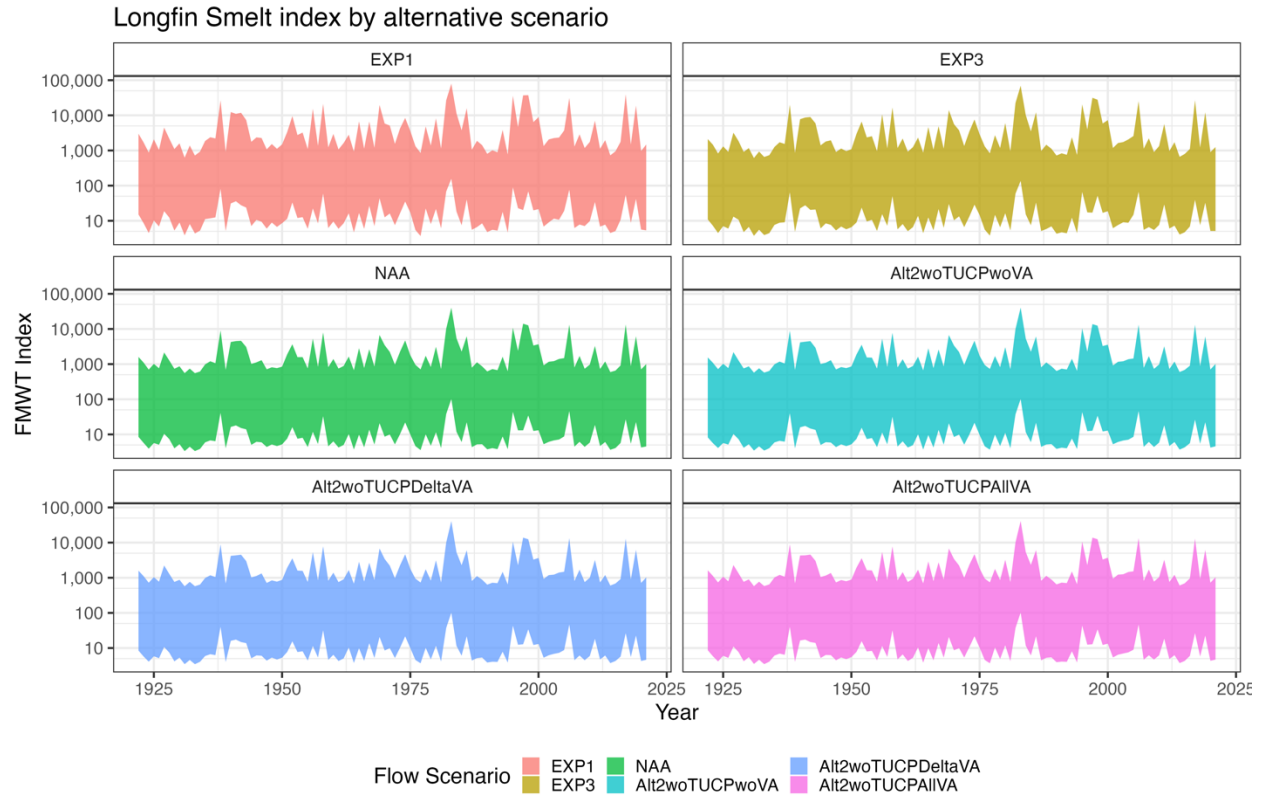


Figure J.1-5. The 95th Bayesian credible intervals for the posterior predictive distributions are shown, based on the parental stock model and the 100 year time series of CalSim 3 Delta Outflow values for each BA scenario.

Longfin Smelt index by alternative scenario

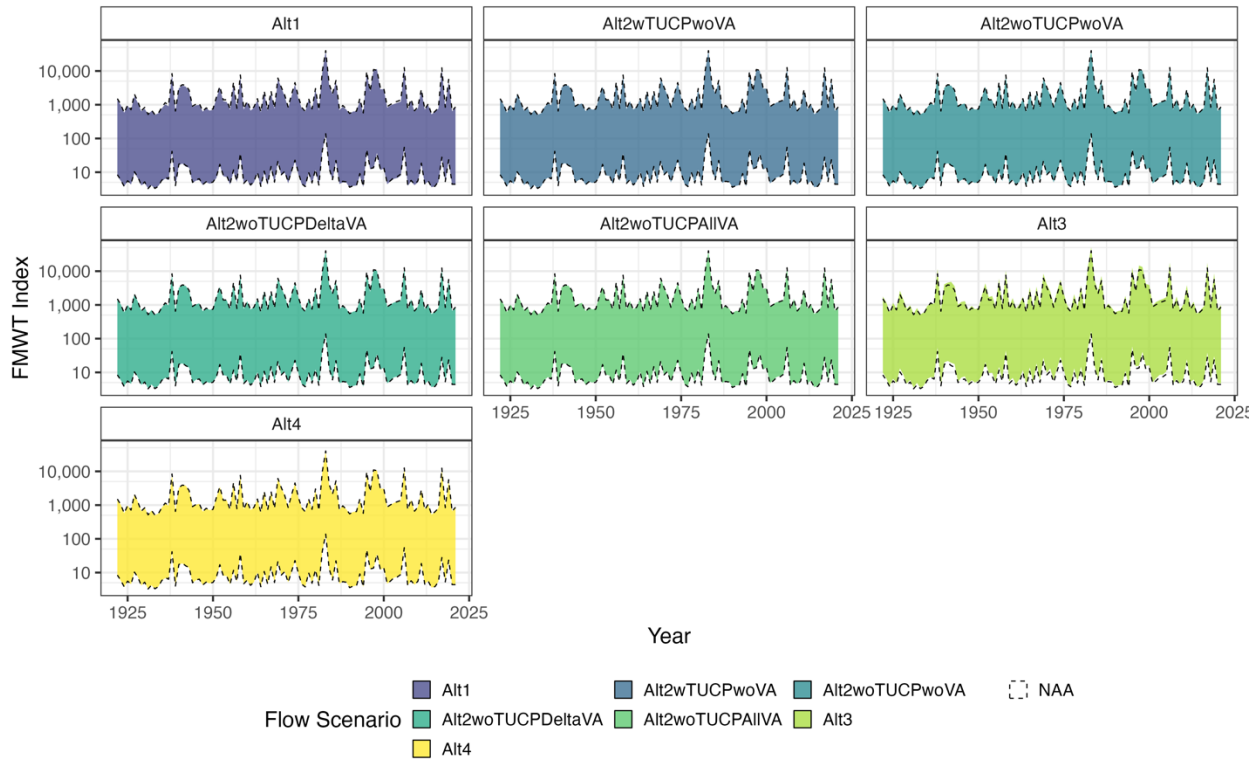


Figure J.1-6. The 95th Bayesian credible intervals for the posterior predictive distributions are shown, based on the parental stock model and the 100 year time series of CalSim 3 Delta Outflow values for each EIS scenario. The credible intervals for the NAA scenario are overlaid as the dashed black lines for comparison with the alternatives.

Longfin Smelt Posterior Predictive Distributions Hypothetical Outflow Comparison

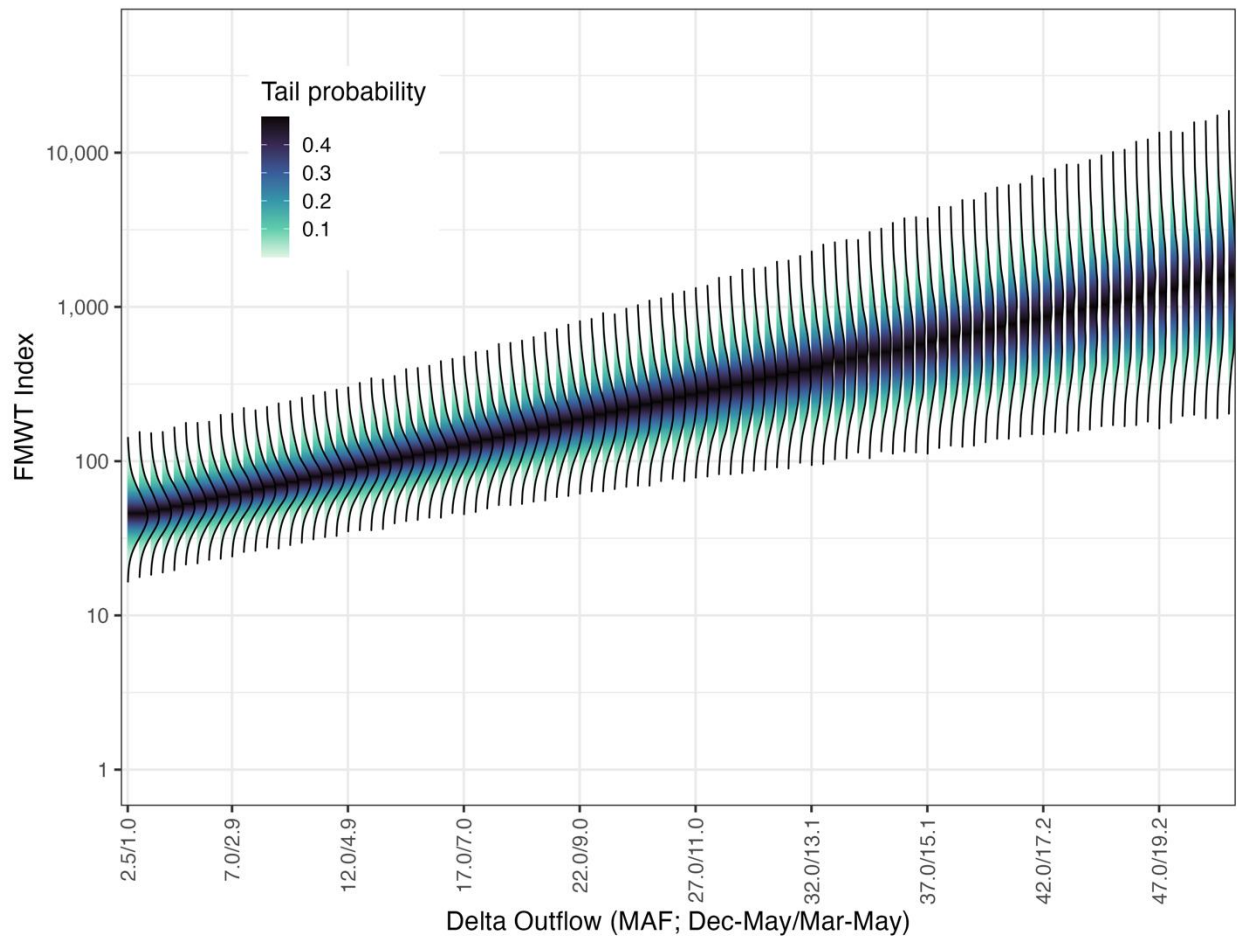


Figure J.1-7. Posterior predictive distributions for the FMWT index are shown as a function of hypothetical outflow levels. The hypothetical outflow levels are paired between the two monthly time periods considered. The paired (Dec-May / Mar-May) values are based on the linear correlation of cumulative outflow values generated from the CalSim 3 runs. "MAF" denotes cumulative outflow across the monthly time periods in million acre-feet.

J.1.4 References

- Bürkner, P.-C. 2017. brms: An R Package for Bayesian Multilevel Models Using Stan. *Journal of Statistical Software* 80(1):1–28.
- Mount, J., W. Fleenor, B. Gray, B. Herbold, and W. Kimmerer. 2013. *Panel Review of the draft Bay-Delta Conservation Plan*. Prepared for the Nature Conservancy and American Rivers. September. Saracino & Mount, LLC, Sacramento, CA.
- Nobriga, M. L., and J. A. Rosenfield. 2016. Population Dynamics of an Estuarine Forage Fish: Disaggregating Forces Driving Long-Term Decline of Longfin Smelt in California's San Francisco Estuary. *Transactions of the American Fisheries Society* 145(1):44–58.
- R Core Team. 2023. *R: A Language and Environment for Statistical Computing*. R Foundation for Statistical Computing, Vienna, Austria. <https://www.R-project.org/>.
- Sommer, T., C. Armor, R. Baxter, R. Breuer, L. Brown, M. Chotkowski, S. Culberson, F. Feyrer, M. Gingras, B. Herbold, W. Kimmerer, A. Mueller-Solger, M. Nobriga, and K. Souza. 2007. The collapse of pelagic fishes in the upper San Francisco Estuary. *Fisheries* 32(6):270–277.
- Vehtari, A., J. Gabry, M. Magnusson, Y. Yao, P. Bürkner, T. Paananen, and A. Gelman. 2020. *loo: Efficient leave-one-out cross-validation and WAIC for Bayesian models*. R package version 2.4.1. Available: <https://mc-stan.org/loo/>. Accessed: May 11, 2022.
- Vehtari, A., A. Gelman, and J. Gabry, 2017. Practical Bayesian model evaluation using leave-one-out cross-validation and WAIC. *Statistics and Computing* 27(5):1413–1432.
- Watanabe, S. 2010. Asymptotic equivalence of Bayes cross validation and widely applicable information criterion in singular learning theory. *Journal of Machine Learning Research* 11:3571–3594.
- Yao, Y., A. Vehtari, D. Simpson, and A. Gelman. 2018. Using Stacking to Average Bayesian Predictive Distributions (with Discussion). *Bayesian Analysis* 13(3):917–1007.

This page intentionally left blank.